Fluorinated Metal–Organic Frameworks: Hydrophobic Nanospaces with High Fluorine Density and Proton Conductivity

Ryota Akai,[a] Hitoshi Kasai,[a] Kouki Oka*[a, b, c]

[a] Institute of Multidisciplinary Research for Advanced Materials,
Tohoku University
2-1-1 Katahira, Aoba-ku, Sendai, Miyagi 980-8577, Japan
E-mail: oka@tohoku.ac.jp (Kouki Oka)

[b] Carbon Recycling Energy Research Center,
Ibaraki University
4-12-1 Nakanarusawa, Hitachi, Ibaraki 316-8511, Japan

[c] Deuterium Science Research Unit, Center for the Promotion of Interdisciplinary Education and Research,
Kyoto University
Yoshida, Sakyo-ku, Kyoto 606-8501, Japan

Experimental Section

1.1 Materials.

Acetic acid was purchased from Nacalai Tesque Inc. (Japan). 2,5-Bis(trifluoromethyl)terephthalic acid, terephthalic acid, and zirconium(IV) chloride were purchased from Tokyo Chemical Industry Co., Ltd. (Japan). 2-(Trifluoromethyl)terephthalic acid was purchased from Combi-Blocks Inc. (USA). Other chemicals were purchased from FUJIFILM Wako Pure Chemical Corporation (Japan).

1.2 Measurements

Microwave-assisted synthesis was performed using the Initiator+ (Biotage, Sweden). Centrifugation was performed using the Centrifuge H-19α (Kokusan, Japan). Fluorine nuclear magnetic resonance (^{19}F NMR) spectra were recorded by a 600 MHz AVANCE III spectrometer (Bruker, America). Field emission scanning electron microscopy (FE-SEM) was performed using a JSM-7800F (JEOL Ltd., Japan); the measurements were carried out at an acceleration voltage of 5 keV and a working distance of 3 mm in USD mode. Powder X-ray diffraction (PXRD) was performed with a SmartLab 3G (Rigaku, Japan) using graphite monochromatized Cu-Kα radiation (λ = 1.5418 Å) at 25°C. Fourier transform infrared (FT-IR) spectra were recorded on a the IRSpirit spectrophotometer (Shimadzu, Japan). Thermogravimetric analysis was performed using the DTG-60A (Shimadzu, Japan) at a heating rate of 1°C min^{-1} under air.

Gas adsorption measurements were performed on a BELSORP-max X (MicrotracBEL, Japan). The adsorption/desorption isotherms for N_2 and H_2O were corrected at 77 K and 298 K, respectively. Before all measurements, the samples were dried under reduced pressure and at 80°C for 3 h.

Proton conductivity testing was performed using pelletized samples pressed in a cylindrical die (surface area: 0.785 cm^2) at 30 MPa for 10 s. The resistance was estimated from the equivalent circuit fitting of Nyquist plots. Proton conductivity was calculated using the equation $\sigma = (1/R)(t/a)$, where σ is the proton conductivity, R is the resistance inside the MOFs, and *t* and *a* are the thickness and area of the pellet, respectively. Alternating current (AC) impedance measurements were performed using the ALS 760E dual electrochemical analyzer (BAS Ltd.) in the frequency range 10^0–10^6 Hz with 0.01 V (amplitude voltage). All measurements were performed at least three times to assure values. The relative humidity (RH) and temperature were controlled using an IW223 incubator (Yamato Scientific, Japan). The resistance value was determined from the equivalent circuit fits of the first semi-circle using the pyZwx software[1]. Direct current (DC) conductivity was determined using a current–potential plot based on the current values obtained upon applying different voltages to the pelletized sample and maintaining them for 60 s.

2.1 Preparation of UiO-66-CF_3

We prepared UiO-66-CF_3 with reference to a previous work[1]. $ZrCl_4$ (150 mg, 0.65 mmol) and 2-(trifluoromethyl)terephthalic acid (151 mg, 0.65 mmol) was dissolved in a solution of *N*,*N*-dimethylformamide (5 mL), acetic acid (1 mL), and water (0.07 mL), and the mixture was sonicated at 20°C for 5 min and stirred at 20°C for 15 min. Finally, the mixture was placed in a microwave oven and irradiated at 120°C for 15 min. The product was centrifuged, then washed with *N*,*N*-dimethylformamide and methanol, and, lastly, dried at 120°C for 5 h, affording a white solid UiO-66-CF_3 (52 mg).

2.2 Preparation of UiO-66-$(CF_3)_2$

$ZrOCl_2 \cdot 8H_2O$ (322 mg, 1.00 mmol) was dissolved in a solution of acetic acid (10 mL) and water (10 mL), and the mixture was sonicated at 20°C for 5 min. Then, 2,5-bis(trifluoromethyl)terephthalic acid (302 mg, 1.00 mmol) was added to the solution and stirred at 20°C for 15 min. Finally, the mixture was placed in a microwave oven and irradiated at 95°C for 15 min. The product was centrifuged at 3500 rpm for 20 min, then washed with water, *N*,*N*-dimethylformamide, and methanol, and, lastly, dried at 120°C for 5 h, affording a yellow solid UiO-66-$(CF_3)_2$ (242 mg).

2.3 Thermogravimetric analysis

As shown in Figure S4, UiO-66 derivatives exhibited three-step weight loss: the first step was caused by water absorbing into the crystal structure, the second step by the dehydration of the Zr clusters, and the third by the linker[2-4]. The combustion reaction (400–500°C) of defect-free UiO-66 is represented by the following equation[2]:

$$Zr_6O_6(C_8H_4O_4)_6 + 45O_2 \rightarrow 6ZrO_2 + 48CO_2 + 12H_2O$$

Theoretically, the normalized weight percentage at 400°C was 220.2%, which led to a 20.03% weight loss per linker. Experimentally, the normalized weight percentage at 400°C was 165.6%. Therefore, the number of linkers containing UiO-66 was calculated as 3.27, *i.e.*, 2.73 linker defect per Zr cluster. Since linker defect sites were occupied by water and hydroxide anions, the molecular weight of UiO-66 was 1282.3 g/mol ($Zr_6O_4(OH)_4(C_8H_4O_4)_{3.27}(H_2O)_{5.46}(OH)_{2.73}$)[4].

Based on the above method, the numbers of linkers containing UiO-66-CF_3 and UiO-66-$(CF_3)_2$ were calculated as 4.58 and 4.21, *i.e.*, 1.42 and 1.79 linker defects per Zr cluster, respectively. Since linker defect sites were occupied by water and hydroxide anions, the molecular weight of UiO-66-CF_3 and UiO-66-$(CF_3)_2$ was 1817.8 g/mol ($Zr_6O_4(OH)_4(C_9H_3O_4F_3)_{4.58}(H_2O)_{2.84}(OH)_{1.42}$) and 2037.8 g/mol ($Zr_6O_4(OH)_4(C_{10}H_2O_4F_6)_{4.21}(H_2O)_{3.58}(OH)_{1.79}$), respectively.

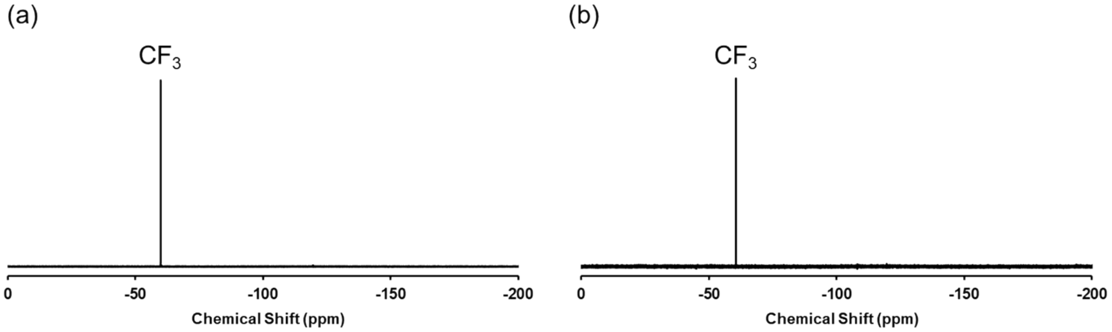

Figure S1. 564 MHz ^{19}F NMR spectra (D_2O) of (a) UiO-66-CF_3 and (b) UiO-66-$(CF_3)_2$.

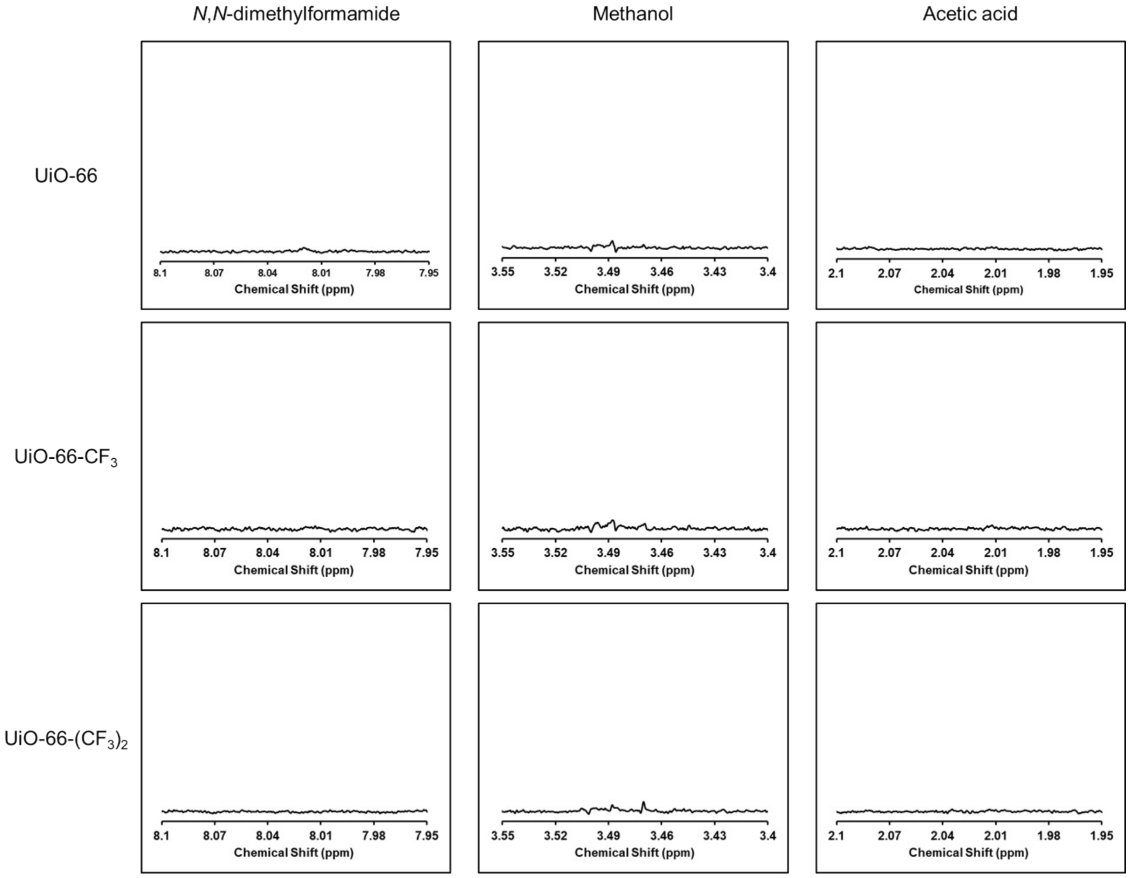

Figure S2. 400 MHz ^{1}H NMR spectra (CDCl$_3$) of UiO-66, UiO-66-CF$_3$, and UiO-66-(CF$_3$)$_2$.

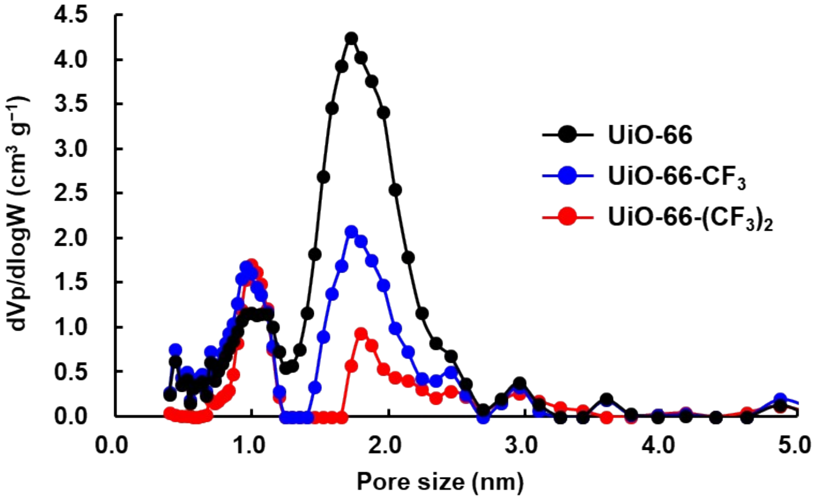

Figure S3. Pore size distributions (volume distribution curves) of UiO-66 (black), UiO-66-CF_3 (blue), and UiO-66-$(CF_3)_2$ (red).

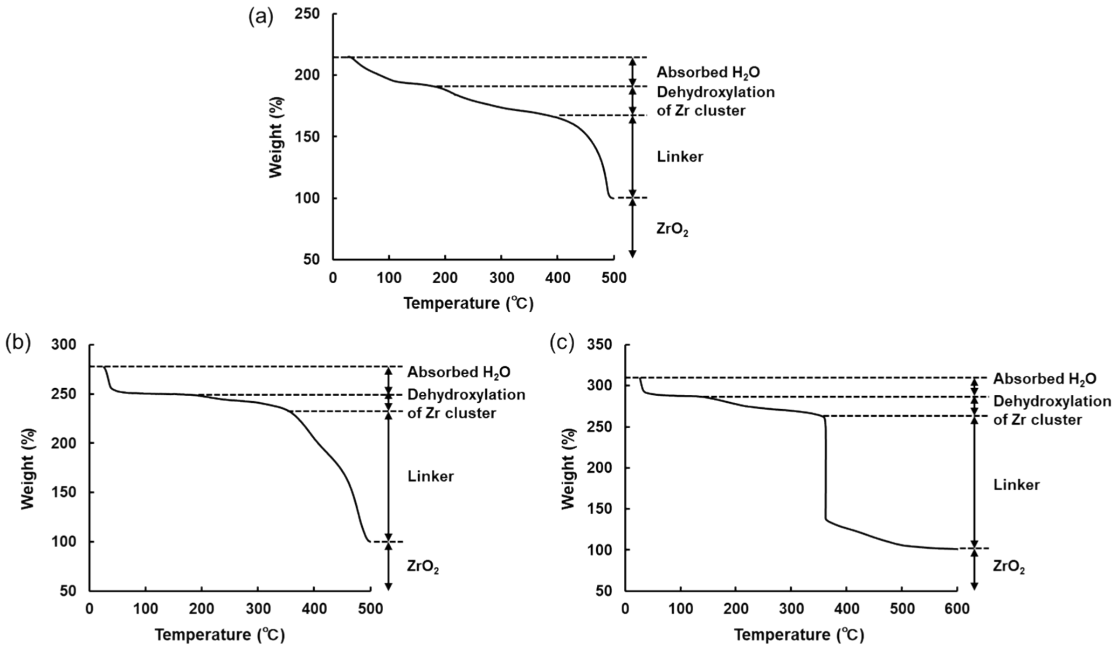

Figure S4. TGA profiles of (a) UiO-66, (b) UiO-66-CF_3, and (c) UiO-66-$(CF_3)_2$ under air.

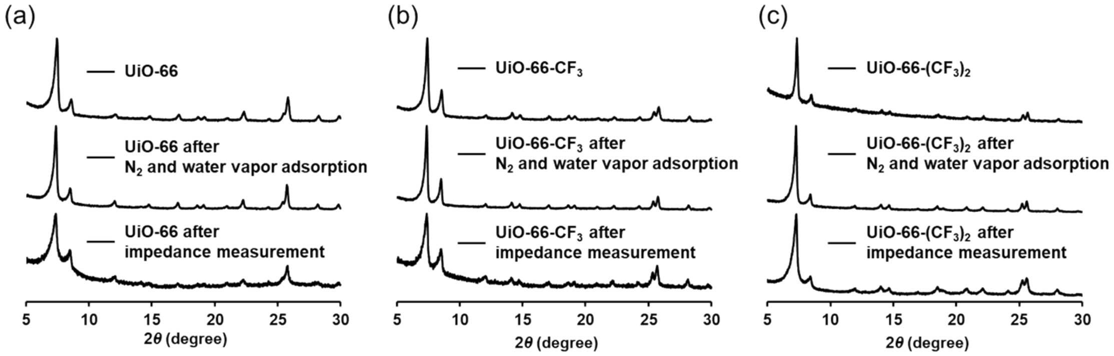

Figure S5. PXRD patterns of (a) UiO-66, (b) UiO-66-CF_3, and (c) UiO-66-$(CF_3)_2$ before (upper) and after N_2 and water vapor adsorption measurement (middle) and after impedance measurement (lower).

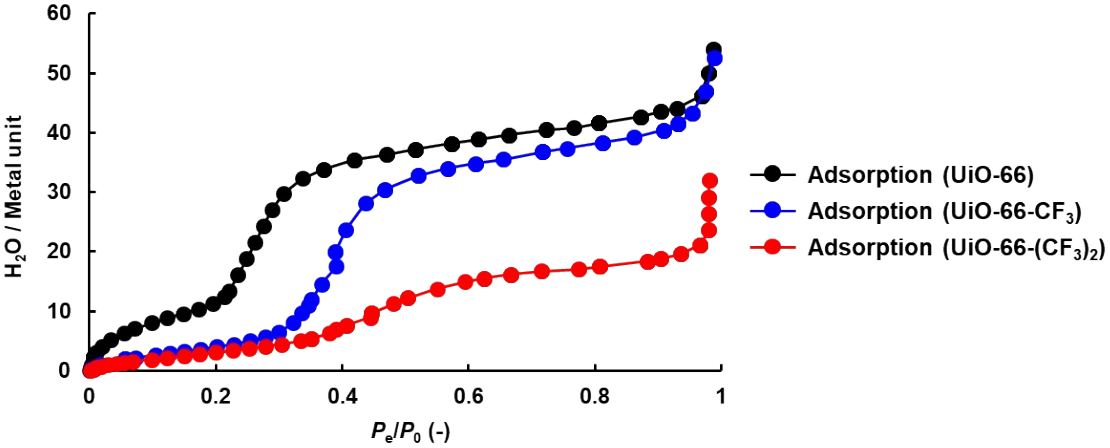

Figure S6. Water vapor adsorption isotherms of UiO-66 (black), UiO-66-CF_3 (blue), and UiO-66-$(CF_3)_2$ (red) at 298 K.

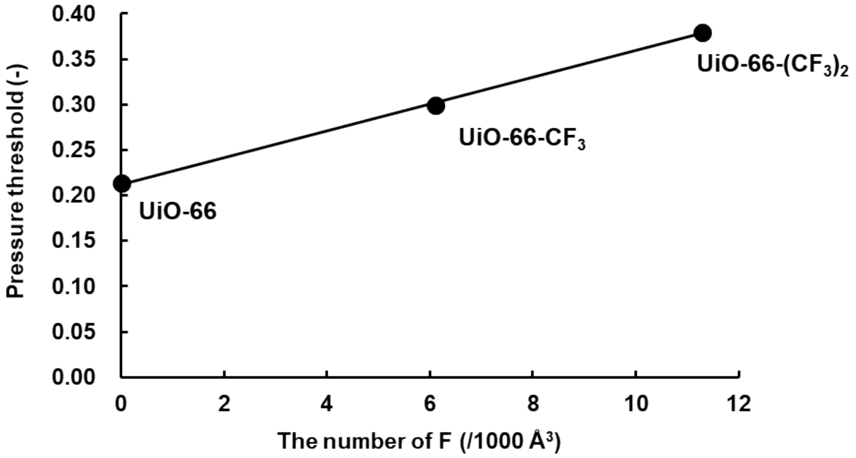

Figure S7. Pressure threshold for the first step of water vapor adsorption depending on the fluorine density of UiO-66-X. Based on the percentage of missing linkers in Experimental Section 2.3, fluorine densities of UiO-66-CF$_3$ and UiO-66-(CF$_3$)$_2$ were calculated to be 6.1 and 11.3 fluorine atoms/1000 Å^3, respectively.

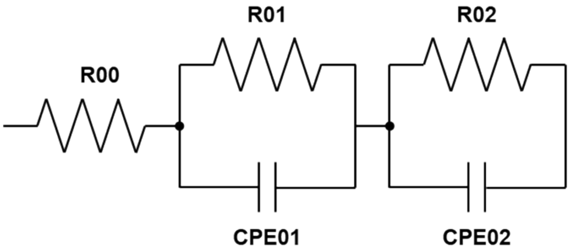

Figure S8. Equivalent circuit for fitting analysis to calculate proton conductivity. The equivalent circuit considered the resistance of cables and bulk and grain boundary resistances in the impedance measurement. Constant-phase element (CPE) was calculated by following the formula $CPE = \{T(i2\pi f)^{\alpha}\}^{-1}\ (0 \le \alpha \le 1, i^2 = -1)$, where T and f were a CPE constant and frequency, respectively.

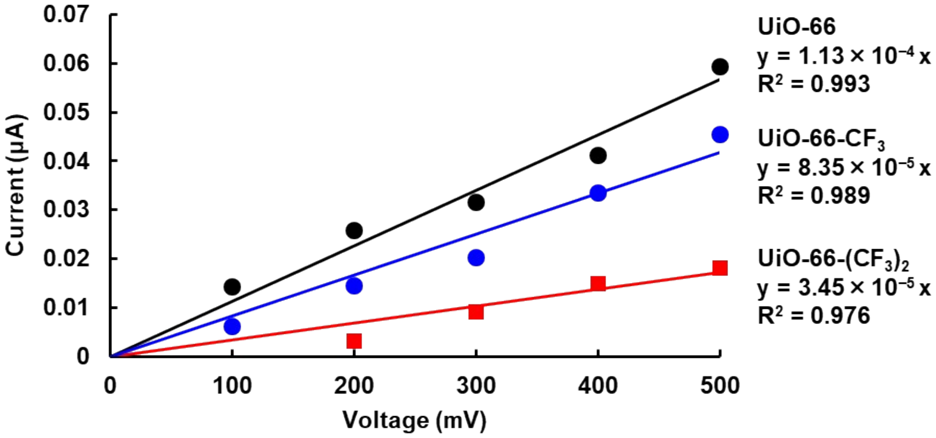

Figure S9. DC electrical conductivity measurement under 95% RH at 30°C of UiO-66 (black), UiO-66-CF_3 (blue), and UiO-66-$(CF_3)_2$ (red).

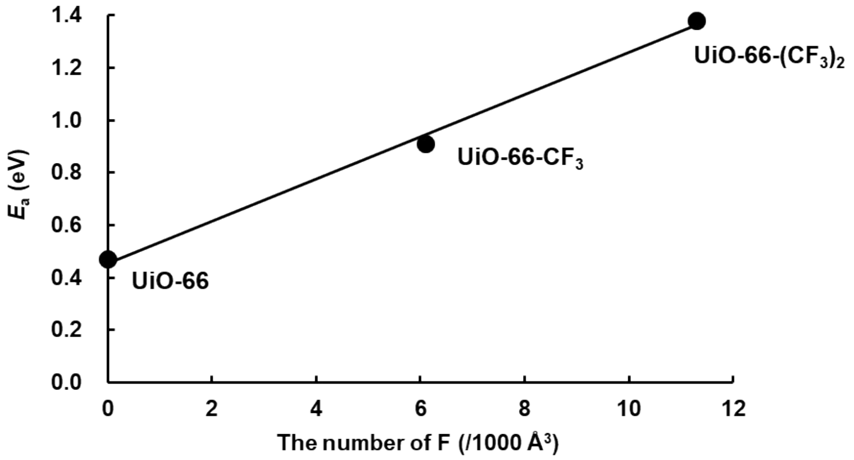

Figure S10. Activation energies (E_a) depending on the fluorine density of UiO-66-X. Based on the percentage of missing linkers in Experimental Section 2.3, fluorine densities of UiO-66-CF$_3$ and UiO-66-(CF$_3$)$_2$ were calculated to be 6.1 and 11.3 fluorine atoms/1000 Å^3, respectively.

Table S1. BET specific surface area and pore volume of UiO-66, UiO-66-CF_3, and UiO-66-$(CF_3)_2$. These values were per Zr cluster.

MOF	BET specific surface area ($\times 10^3$ m^2 mol^{-1})	Pore volume[a] (cm^3 mol^{-1})
UiO-66	2143	2220
UiO-66-CF_3	1825	1836
UiO-66-$(CF_3)_2$	970	395

[a] Calculated based on the non-local density functional theory/grand canonical Monte Carlo (NLDFT/GCMC) method.

Table S2. Assignments of FT-IR spectra in Figure 2c.

Assignments	Wavenumber (nm^{-1})
COO^- stretching	1610, 1410, 1363, 1067
C=C stretching	1520
C–F stretching	1300, 1273, 1140
C–H bending	909, 744
Zr–$O_{\mu 3-O}$ stretching	661
Zr–(OC) stretching	970

References

1. M. Taddei, P. V. Dau, S. M. Cohen, M. Ranocchiari, J. A. van Bokhoven, F. Costantino, S. Sabatini and R. Vivani, *Dalton Trans.*, 2015, **44**, 14019-14026.
2. J. Winarta, B. Shan, S. M. McIntyre, L. Ye, C. Wang, J. Liu and B. Mu, *Cryst. Growth Des.*, 2020, **20**, 1347-1362.
3. J. M. Taylor, S. Dekura, R. Ikeda and H. Kitagawa, *Chem. Mater.*, 2015, **27**, 2286-2289.
4. C. A. Trickett, K. J. Gagnon, S. Lee, F. Gándara, H.-B. Bürgi and O. M. Yaghi, *Angew. Chem., Int. Ed.*, 2015, **54**, 11162-11167.